Available online at www.sciencedirect.com
ScienceDirect
Trans. Nonferrous Met. Soc. China 32(2022) 3250−3258
Transactions of Nonferrous Metals Society of China
www.tnmsc.cn

Electroplated super-hydrophobic Zn−Fe coating for corrosion protection on magnesium alloy

Xue MENG[1], Jin-lei WANG[1], Jie ZHANG[1,2], Bao-long NIU[1,2], Xiang-hua GAO[1,2], Hong YAN[1,2]

1. College of Materials Science and Engineering, Taiyuan University of Technology, Taiyuan 030024, China;
2. Key Laboratory of Interface Science and Engineering in Advanced Materials, Ministry of Education, Taiyuan University of Technology, Taiyuan 030024, China

Received 26 August 2021; accepted 22 March 2022

Abstract: A superhydrophobic Zn−Fe alloy coating was prepared on the surface of a reactive magnesium alloy using a simple, low-cost, eco-friendly method. Firstly, the Zn−Fe coating was obtained in a neutral glycerol Zn−Fe plating solution, which is green, compositionally stable, and non-corrosive to the equipment. And then the superhydrophobic surface with a flower-like microstructure was obtained by grafting myristic acid onto the Zn−Fe coating via a chelation reaction. The water contact angle was >150° and the rolling angle was 3°−4°. The corrosion rate of the two groups of superhydrophobic magnesium alloy samples with electrodeposition time of 30 and 50 min, respectively, was reduced by about 87% compared to that of the bare magnesium alloy. The prepared superhydrophobic coatings exhibit high performance in self-cleaning, abrasion resistance, and corrosion resistance.

Key words: Zn−Fe coating; Mg alloy; contact angle; sliding angle; self-cleaning; abrasion resistance

1 Introduction

Magnesium alloy is the lightest metal material that we have known at present [1,2]. It has a series of advantages such as high specific strength, low density, high specific modulus of elasticity, good electromagnetic shielding properties, shock absorption, heat dissipation, biocompatibility, and easy recycling [3,4]. Magnesium is an earth-abundant element, but due to its extremely active chemical nature, it is highly susceptible to oxidation and corrosion. Therefore, it is significant to improve the corrosion resistance of magnesium alloy [5,6].

Inspired by the "lotus effect", super-hydrophobic materials have an extremely wide range of promising applications, such as marine transportation, outdoor snow-proof antennas, oil pipelines, outdoor window self-cleaning, textile panels, solar panels, and many other fields [7−9]. Superhydrophobic surfaces have attracted much attention because of their excellent properties [10].

Thus, creating a superhydrophobic surface on magnesium alloys can prevent them from corrosion in wet environments [11−13]. The main method to prepare superhydrophobic coatings is to fabricate micro/nano structures on the substrate surface, followed by the modification with low surface energy substances [14]. JIANG et al [15] obtained micro/nano-structured surfaces on copper plates by simple one-step pulsed electrodeposition. LIU et al [16] prepared superhydrophobic surfaces on AZ91D magnesium alloy by electrodeposition and stearic acid modification.

Zinc alloy (Zn−X, X denoting Fe, Ni, and other iron group elements) coating is a common sacrificial anode to protect other metals from corrosion [17]. However, nickel causes skin sensitization, such as dermatitis, thus endangering

Corresponding author: Hong YAN, E-mail: yanhong@tyut.edu.cn
DOI: 10.1016/S1003-6326(22)66017-5

human health [18]. More improvements are required for fabricating a superhydrophobic coating in terms of environmental protection, human health, economic applicability, fast preparation, and durability [19]. Therefore, zinc−iron plating, which is not harmful to human health, was chosen for this study. Some studies have shown that Zn−Fe coating has better corrosion resistance than pure zinc coating [20,21].

In this study, we proposed a cost-efficient and eco-friendly process to prepare superhydrophobic Zn−Fe coating on magnesium alloy by constant potential electrodeposition in a neutral glycerol electrolyte and by surface modification with fluorine-free myristic acid. Moreover, the superhydrophobic coating possesses excellent corrosion and wear resistance, as well as self-cleaning performance.

2 Experimental

2.1 Materials and chemicals

AZ31B magnesium alloy and zinc sheet were purchased from the local chemical market. AZ31B magnesium alloy was cut to the size of 20 mm × 10 mm × 2 mm. The zinc sheet was twice the size of the AZ31B magnesium alloy sample. Anhydrous ethanol, acetone, ferrous sulfate, zinc chloride, sodium hydroxide, and glycerol were purchased from Tianjin Damao Chemical Reagent Factory, China. Myristic acid used in the experiment was purchased from Shanghai Maclean Biochemical Co., Ltd., China. All chemicals were analytical reagents, and the solutions were prepared with deionized water.

2.2 Preparation of superhydrophobic Zn−Fe coating

The magnesium alloy was polished with SiC sandpaper (400, 800, 1200, and 2000 grit) to remove the oxide layer and rust spots on the surface. The polished magnesium alloy samples were ultrasonically cleaned with acetone and anhydrous ethanol for 5 min, respectively, and then dried at room temperature. The pretreated magnesium alloy samples were made into electrodes with 704 silicone sealant. The pretreated magnesium alloy was used as a cathode, and the zinc sheet was used as an anode. A 100 mL of electrolyte contained 0.2 mol/L Zn^{2+} and 0.1 mol/L Fe^{2+}. Glycerol accounted for two-thirds of the total volume of the solution, and the pH value of the solution was adjusted to 7−8 with sodium hydroxide solution. The electrodeposition was carried out at 7 V for 30 or 50 min. The obtained samples were rinsed several times with deionized water. Then, the obtained magnesium alloy samples were soaked in a myristic acid-dissolved anhydrous ethanol solution (0.1 mol/L) for 8 h. Finally, the superhydrophobic samples were taken out, rinsed with anhydrous ethanol, and dried at room temperature.

2.3 Characterization

The surface morphology and elemental distribution of the superhydrophobic magnesium alloys were characterized by field emission scanning electron microscopy (FESEM) and energy-dispersive X-ray spectroscopy (EDS). An X-ray photoelectron spectrometer (Thermo Fischer, ESCALAB 250Xi, USA) was used for the surface chemical analysis of the superhydrophobic magnesium alloy. An optical contact angle measuring instrument (JC2000C1, Shanghai Centron Digital Technology Co., Ltd., China) was used to measure the water contact angle by the goniometric method. Electrochemical workstation (CorrTest CS Studio 5.3) was used for plating and corrosion protection performance testing.

3 Results and discussion

3.1 Surface morphology and chemical composition

Figure 1 shows the morphology of superhydrophobic surfaces. The superhydrophobic coatings were uniform and dense. A longer plating time caused a thicker and denser coating. As shown in Figs. 1(c) and (f), the coatings exhibited flower-like micro/nano structures, enabling more air to be trapped on the surface [22−24].

EDS mappings in Fig. 2 present that elemental C, O, Zn and Fe are uniformly distributed on the surface of two coatings. Elements C and O cover elements Zn and Fe, indicating that myristic acid was chelated on the surface of the Zn−Fe coating. This uniform distribution is crucial to achieving its excellent performance such as self-cleaning and anti-corrosion.

The superhydrophobic coating plated for 50 min was investigated using XPS. The full-survey

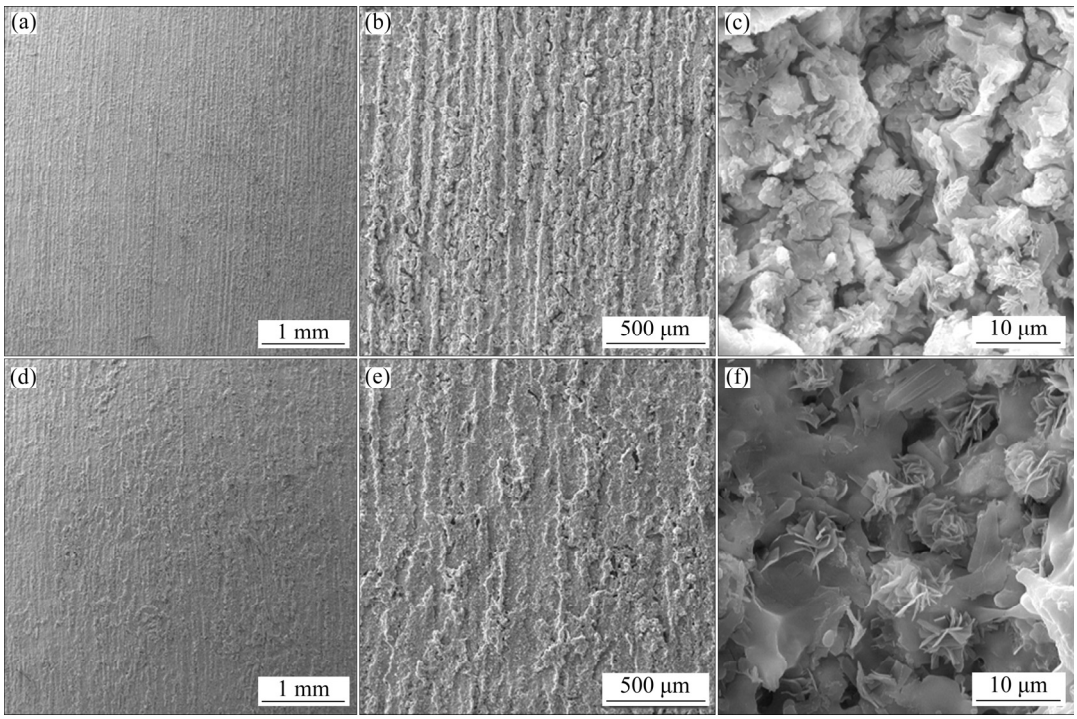

Fig. 1 SEM images of superhydrophobic coatings plated for 30 min (a–c) and 50 min (d–f)

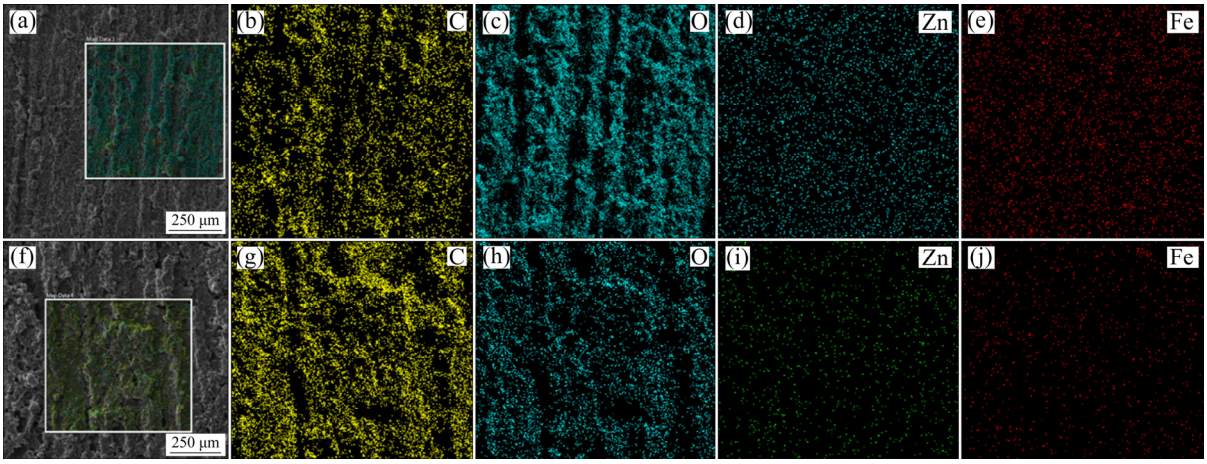

Fig. 2 EDS mappings of superhydrophobic coatings plated for 30 min (a–e) and 50 min (f–j)

XPS spectrum (Fig. 3(a)) of the superhydrophobic surface shows that the contents (molar fractions) of C and O are much higher than those of Fe and Zn, indicating that myristic acid covers the Zn–Fe coating.

Figures 3(b–e) show high-solution spectra of C 1s, O 1s, Zn 2p, and Fe 2p, respectively. For C 1s spectrum (Fig. 3(b)), —O═C—O (288.4 eV), —CH_3 (285.3 eV) and —CH_2 (284.6 eV) were identified [25]. They all originated from the myristic acid chelated to metals. In the O 1s spectrum (Fig. 3(c)), —C═O— (532.4 eV) and —C—O— (531.6 eV) were derived from $CH_3(CH_2)_{12}COO$—, while M—O— (531.1 eV) was from Zn—O and Fe—O [26]. This further confirms the formation of tetradecanoate. Besides, as shown in Fig. 3(d), the binding energies of the main Zn $2p_{3/2}$ and Zn $2p_{1/2}$ are around 1022 and 1045 eV, respectively, with a spin-orbit coupling energy gap of 23.0 eV [27,28]. The results indicate that Zn^{2+} is the main valence state of zinc. Lastly, as shown in Fig. 3(e), since Fe has lower content than Zn, its XPS scan signal is very weak, thus its valence state was not discussed here [29].

3.2 Superhydrophobicity and self-cleaning performance

Figure 4 shows the contact angles of different

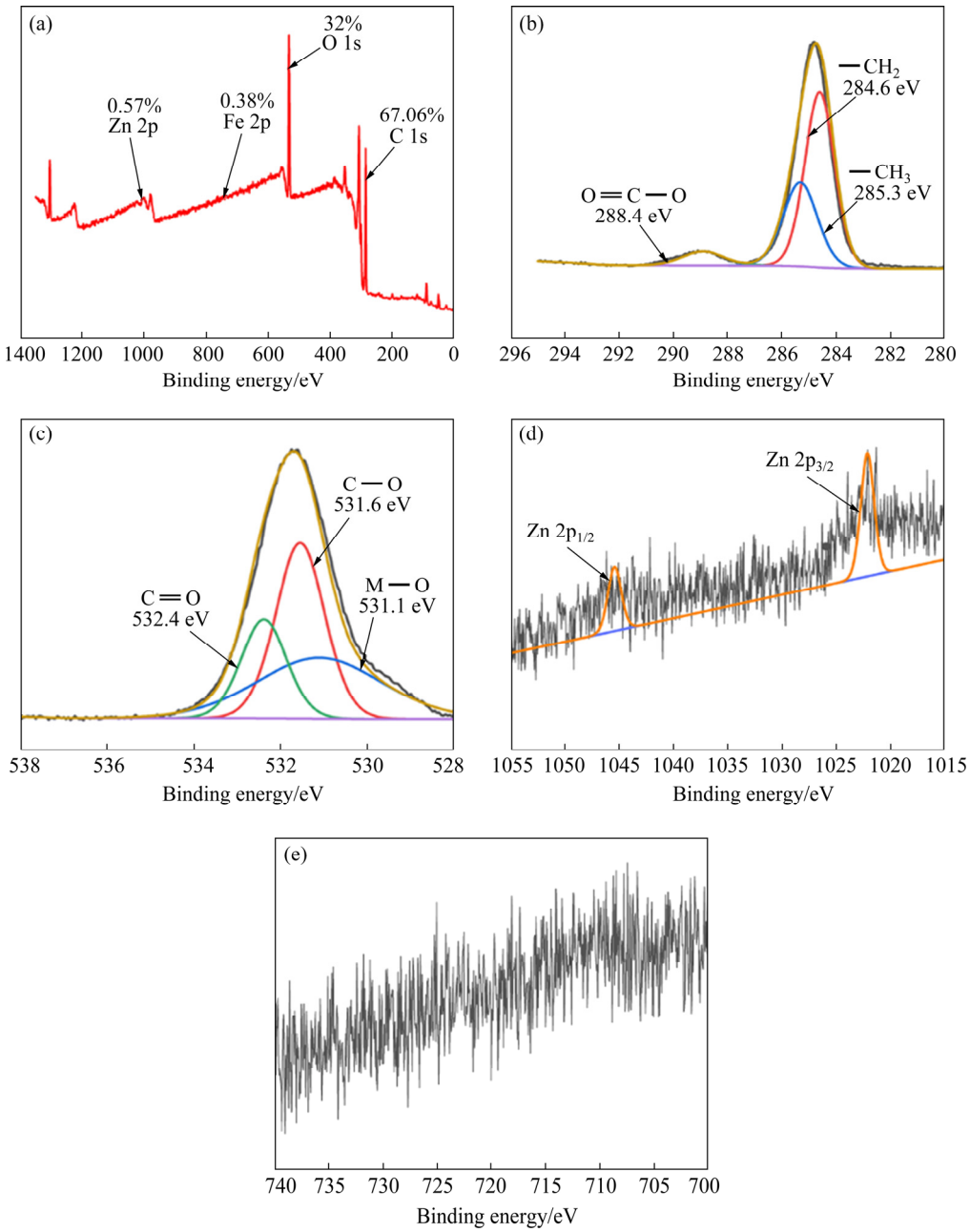

Fig. 3 XPS spectra of superhydrophobic coating plated for 50 min: (a) Full survey; (b) C 1s; (c) O 1s; (d) Zn 2p; (e) Fe 2p

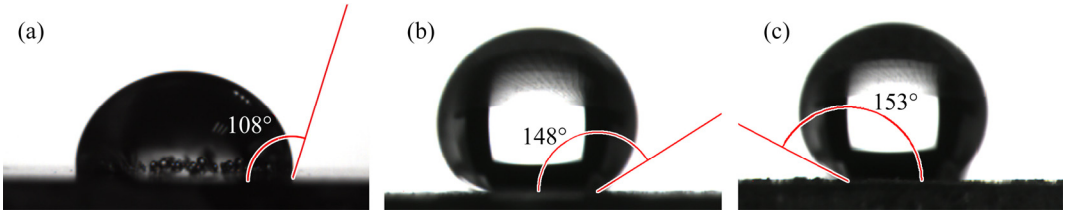

Fig. 4 Water contact angles of different samples: (a) Bare magnesium alloy; (b, c) Superhydrophobic magnesium alloys plated for 30 min (b) and 50 min (c)

samples measured at room temperature by the goniometric method, using a 10 μL water droplet. The contact angles of two superhydrophobic samples are 148° (30 min) and 153° (50 min), which are much higher than that of the bare magnesium alloy (108°).

The rolling angle of water droplet on the superhydrophobic surface is required to be less than 10° [30]. The rolling angles of two superhydrophobic surfaces, as shown in Figs. 5(b) and (d), are 4° (30 min) and 3° (50 min), indicating a good superhydrophobic effect.

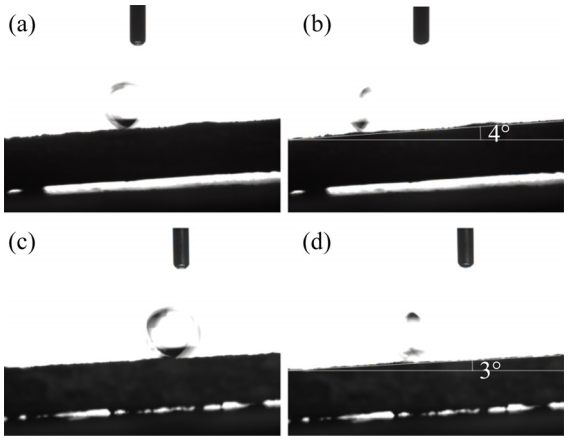

Fig. 5 Rolling motion of water droplets on surfaces of superhydrophobic magnesium alloys plated for 30 min (a, b) and 50 min (c, d)

Blue chalk dust was selected as the contamination particles. Two superhydrophobic samples were placed on an inclined surface, a certain amount of blue chalk dust was sprinkled on the surfaces of samples, and deionized water was continuously dropped from a dropper to test whether the blue chalk dust would be carried away by the water droplets [31,32]. Figure 6 shows that the water droplets successfully removed the fine blue chalk dust, indicating that two samples have excellent self-cleaning performance [33]. The uniform micro/nano structure of the obtained superhydrophobic coating contributes to excellent self-cleaning performance.

3.3 Corrosion resistance

The dynamic potential polarization and electrochemical impedance spectroscopy (EIS) tests were performed in 3.5 wt.% NaCl solution by an electrochemical workstation at room temperature. A classical three-electrode cell was constructed with a platinum plate as the counter electrode, a saturated glycerol electrode (SCE) as the reference electrode, and a superhydrophobic magnesium alloy sample as the working electrode. Before the test, the sample was immersed in 3.5 wt.% NaCl solution for 10 min to obtain a stable open-circuit voltage.

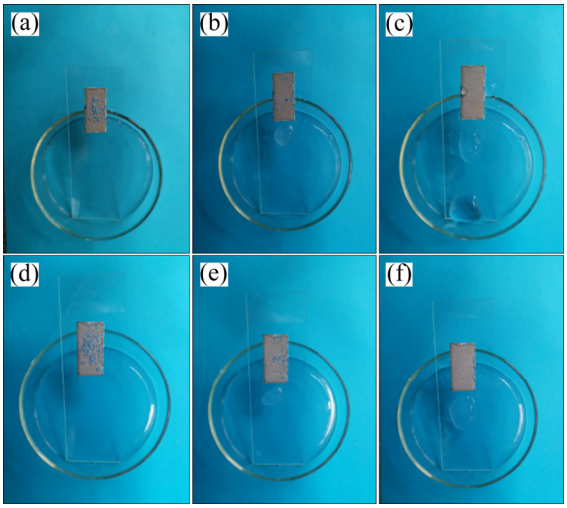

Fig. 6 Self-cleaning test results of superhydrophobic magnesium alloys plated for 30 min (a−c) and 50 min (d–f)

Figure 7(a) shows the Nyquist plots for the three sets of samples. Except for the semicircle diameter, the electrochemical impedance spectra of the three groups of samples showed similar trend, indicating that they have the same corrosion mechanism and different corrosion rates. The high-frequency semicircle in the Nyquist plot represents the charge transfer resistance at the solid−liquid interface, and the diameter of the semicircle impedance arc represents the polarization resistance. The superhydrophobic magnesium alloy sample (50 min) has higher charge transfer and polarization resistances, indicating a better corrosion resistance [34−37].

Figure 7(b) shows the Bode plots of impedance modulus and frequency for three sets of magnesium alloy samples. For all samples, the Bode plots of impedance modulus and frequency show three-time constants corresponding to the charge transfer constant in the high-frequency region, the corrosion resistance of the coating in the medium frequency region, and the capacitive susceptibility loop in the low-frequency region [34,36,37]. The superhydrophobic magnesium alloy sample (50 min) has the highest impedance modulus $|Z|$ in the low-frequency region, indicating that thicker coating has better corrosion resistance in the corrosive environment.

Figure 7(c) presents the Bode plots of phase angle versus frequency for the three sets of magnesium alloy samples. The impedance

performance of the magnesium alloy (50 min) is the best because it has the highest phase angle in the high-frequency region [34,36,37].

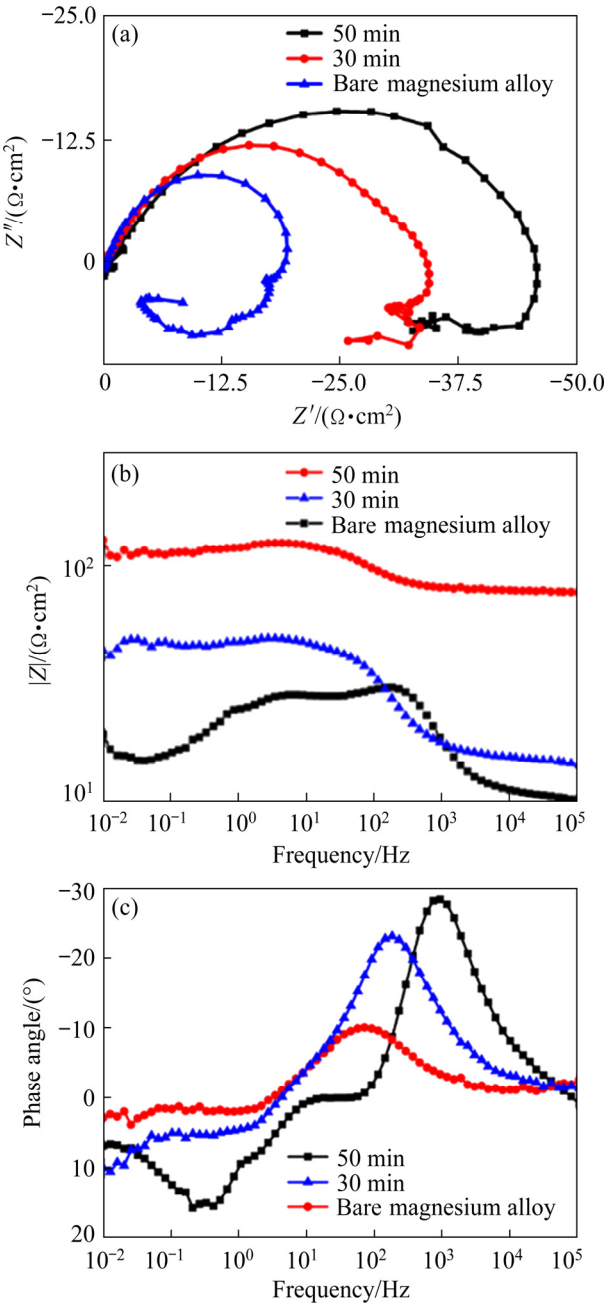

Fig. 7 EIS test results for different samples: (a) Nyquist plots; (b) Bode plots of $|Z|$ versus frequency; (c) Bode plots of phase angle versus frequency

After the electrochemical impedance spectroscopy test was completed, the scan rate was set to be 5 mV/s for dynamic polarization curve tests. The initial potential was set to be −2.5 V and the termination potential was set to be 0.1 V.

The dynamic potential polarization curves of the three sets of magnesium alloys are shown in Fig. 8.

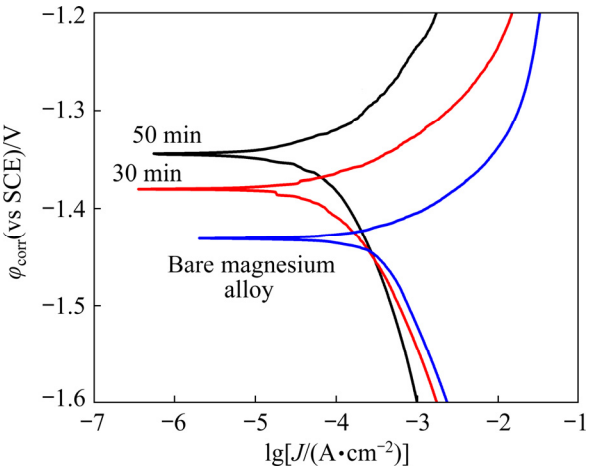

Fig. 8 Dynamic potential polarization curves of different samples in 3.5 wt.% NaCl solution

The electrochemical analysis software (CorrView) was used to characterize the corrosion resistance of the coatings. The Tafel extrapolation method can be used to obtain the corrosion potential (φ_{corr}), corrosion current (J_{corr}), Tafel slopes of the anodic and cathodic polarization (β_a and β_c), and the corrosion rate (CR). Table 1 shows the results of the Tafel fitting of the dynamic polarization curves for the three sets of samples.

The corrosion rates of the two groups of superhydrophobic magnesium alloy samples with electrodeposition time of 30 and 50 min, were reduced by about 87% compared to that of the bare magnesium alloy. In general, the smaller the corrosion current and the higher the corrosion potential are, the better the corrosion resistance of

Table 1 Corrosion parameters calculated by Tafel extrapolation method for different samples

Sample	β_a/(mV·dec^{-1})	β_c/(mV·dec^{-1})	φ_{corr}/V	J_{corr}/(A·cm^{-2})	CR/(mm·a^{-1})
Bare magnesium alloy	92.889	578.41	−1.431	7.9601×10^{-4}	17.388
30 min	69.437	172.58	−1.3803	1.1481×10^{-4}	2.508
50 min	106.68	214.55	−1.3448	9.3679×10^{-5}	2.0463

the material under test is. Compared with the influence of corrosion potential on corrosion performance, the influence of corrosion current is greater [34−37]. As shown in Table 1, the corrosion current density of the super-hydrophobic magnesium alloy sample (50 min) is the smallest and the corrosion rate is the smallest, which indicates its excellent corrosion resistance.

3.4 Abrasion resistance

For a long time, artificially prepared superhydrophobic surfaces have had low abrasion resistance, which greatly limits the application of superhydrophobic surfaces in practice [38]. Thus, we tested the abrasion resistance of the super-hydrophobic coatings plated for 30 and 50 min, respectively. As shown in Fig. 9, the samples were placed on the 2000 grit sandpapers under 2.45 kPa, and were then moved on the sandpaper for 1 m with the help of a tweezer.

It can be seen from Fig. 10 that the contact angles of the two groups of samples did not decrease significantly during the gradual increase of the friction distance from 100 to 900 mm. Until the friction distance reaches 1000 mm, the contact angle decreases significantly. This indicates that the surface-long alkyl chain has disappeared at this time. In conclusion, the abrasion resistance of the superhydrophobic coating reaches a distance of nearly 1 m on sandpaper with a roughness of 2000 grit at a pressure of 2.45 kPa.

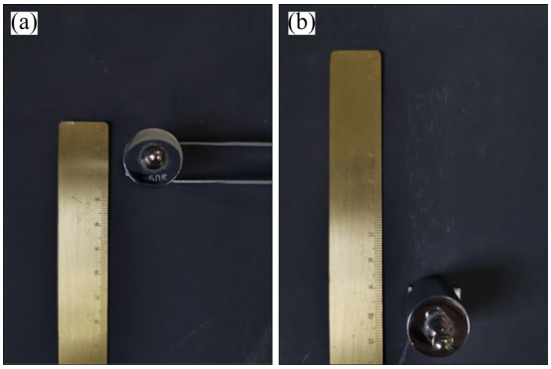

Fig. 9 Abrasion resistance test process of super-hydrophobic magnesium alloy: (a) Start of test; (b) Test in progress

4 Conclusions

(1) A method was proposed to prepare a superhydrophobic surface on magnesium alloy by one-step electroplating using glycerol Zn−Fe electrolyte and tetradecanoic acid immersion. This preparation method of superhydrophobic Zn−Fe coating is simple, economical and eco-friendly, which is promising in large-scale industrial production.

(2) The superhydrophobic Zn−Fe coating exhibits flower-like micro/nano structure, good self-cleaning performance and abrasion resistance. Due to the barrier and super-hydrophobic effects of the coating, the corrosion rate of the magnesium alloy substrate was reduced by 87%.

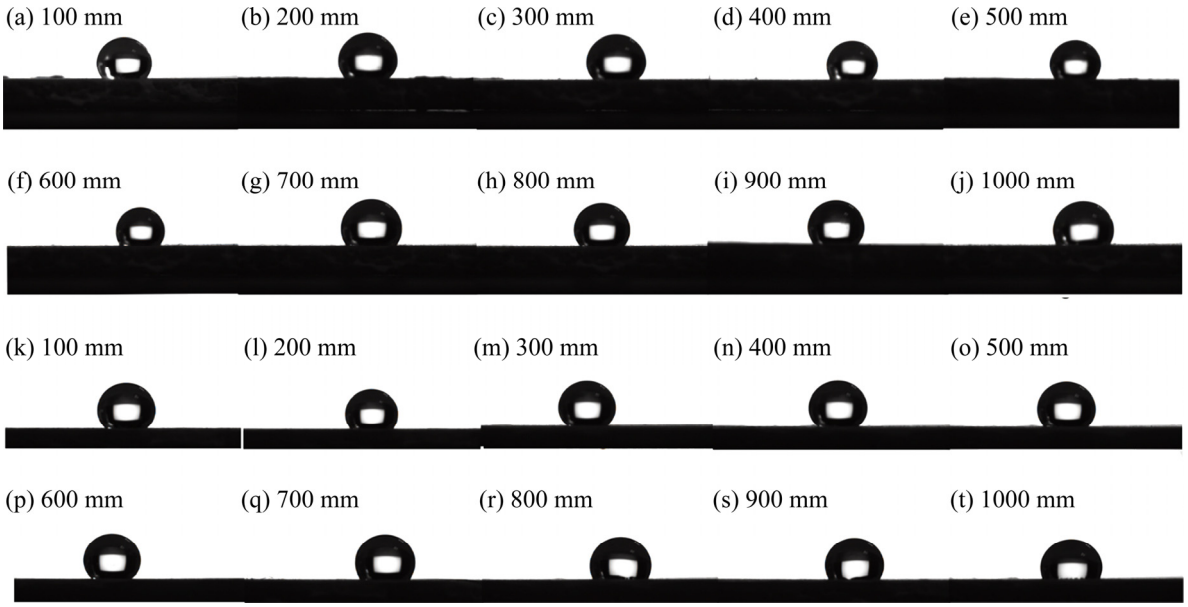

Fig. 10 Variation of contact angle during abrasion resistance tests for superhydrophobic magnesium alloys plated for 30 min (a−j) and 50 min (k−t)

Acknowledgments

The authors are grateful for the financial supports from the National Natural Science Foundation of China (No. 22178242).

References

[1] WANG X, JING C, CHEN Y X, WANG X S, ZHAO G, ZHANG X, WU L, LIU X Y, DONG B Q, ZHANG Y X. Active corrosion protection of super-hydrophobic corrosion inhibitor intercalated Mg−Al layered double hydroxide coating on AZ31 magnesium alloy [J]. Journal of Magnesium and Alloys, 2020, 8(1): 291−300.

[2] CHEN J L, FANG L, WU F, ZENG X G, HU J, ZHANG S F, JIANG B, LUO H J. Comparison of corrosion resistance of MgAl−LDH and ZnAl−LDH films intercalated with organic anions ASP on AZ31 Mg alloys [J]. Transactions of Nonferrous Metals Society of China, 2020, 30(9): 2424−2434.

[3] HAN B J, YANG Y, FANG L, PENG G H, YANG C B. Electrodeposition of super-hydrophobic nickel film on magnesium alloy AZ31 and its corrosion resistance [J]. International Journal of Electrochemical Science, 2016, 11(11): 9206−9215.

[4] QIU Z M, ZENG R C, ZHANG F, SONG L, LI S Q. Corrosion resistance of Mg−Al LDH/Mg(OH)$_2$/silane−Ce hybrid coating on magnesium alloy AZ31 [J]. Transactions of Nonferrous Metals Society of China, 2020, 30(11): 2967−2979.

[5] YIN B, FANG L, HU J, TANG A Q, WEI W H, HE J. Preparation and properties of super-hydrophobic coating on magnesium alloy [J]. Applied Surface Science, 2010, 257(5): 1666−1671.

[6] SHI L T, HU J, LIN X D, FANG L, WU F, XIE J, MENG F M. A robust superhydrophobic PPS−PTFE/SiO_2 composite coating on AZ31 Mg alloy with excellent wear and corrosion resistance properties [J]. Journal of Alloys and Compounds, 2017, 721: 157−163.

[7] LI J H, LIU Q, WANG Y L, CHEN R R, TAKAHASHI K, LI R M, LIU L H, WANG J. Formation of a corrosion-resistant and anti-icing superhydrophobic surface on magnesium alloy via a single-step method [J]. Journal of the Electrochemical Society, 2016, 163(5): C213−C220.

[8] VAZIRINASAB E, JAFARI R, MOMEN G. Application of superhydrophobic coatings as a corrosion barrier: A review [J]. Surface and Coatings Technology, 2018, 341: 40−56.

[9] WANG L, YANG J Y, ZHU Y, LI Z H, SHENG T, HU Y M, YANG D Q. A study of the mechanical and chemical durability of ultra-ever dry superhydrophobic coating on low carbon steel surface [J]. Colloids and Surfaces A: Physicochemical and Engineering Aspects, 2016, 497: 16−27.

[10] ISHIZAKI T, MASUDA Y, SAKAMOTO M. Corrosion resistance and durability of superhydrophobic surface formed on magnesium alloy coated with nanostructured cerium oxide film and fluoroalkylsilane molecules in corrosive NaCl aqueous solution [J]. Langmuir, 2011, 27(8): 4780−4788.

[11] CHOBAOMSUP V, METZNER M, BOONYONG-MANEERAT Y. Superhydrophobic surface modification for corrosion protection of metals and alloys [J]. Journal of Coatings Technology and Research, 2020, 17(3): 583−595.

[12] MA N, CHEN Y, ZHAO S G, LI J C, SHAN B F, SUN J H. Preparation of super-hydrophobic surface on Al−Mg alloy substrate by electrochemical etching [J]. Surface Engineering, 2019, 35(5): 394−402.

[13] XIONG J W, SARKAR D K, CHEN X G. Superhydrophobic honeycomb-like cobalt stearate thin films on aluminum with excellent anti-corrosion properties [J]. Applied Surface Science, 2017, 407: 361−370.

[14] DU X Q, CHEN Y. Corrosion inhibition by a super-hydrophobic surface on aluminum that was prepared with a facile electrochemical route [J]. Materials Research Express, 2020, 7(5): 056405.

[15] JIANG S Z, GUO Z N, GYIMAH G K, ZHANG C Y, LIU G X. Preparation of biomimetic superhydrophobic surface by a facile one-step pulse electrodeposition [J]. Procedia CIRP, 2018, 68: 237−241.

[16] LIU Y, YIN X M, ZHANG J J, YU S R, HAN Z W, REN L Q. A electro-deposition process for fabrication of biomimetic super-hydrophobic surface and its corrosion resistance on magnesium alloy [J]. Electrochimica Acta, 2014, 125: 395−403.

[17] THANGARAJ V, RAVISHANKAR K, CHITHARANJAN HEGDE A. Surface modification by compositionally modulated multilayered Zn−Fe alloy coatings [J]. Chinese Journal of Chemistry, 2008, 26(12): 2285−2291.

[18] PYRKOV S T, POGODIN V S, PODKIN I S. The interrelation between allergic reactions to dentures made of stainless steel and the skin hypersensitivity to Cr and Ni [J]. Stomatologiia, 1991(6): 41−42.

[19] QIAN Z Q, WANG S D, YE X S, LIU Z, WU Z J. Corrosion resistance and wetting properties of silica-based superhydrophobic coatings on AZ31B Mg alloy surfaces [J]. Applied Surface Science, 2018, 453: 1−10.

[20] PUNITH KUMAR M K, REKHA M Y, AGRAWAL J, AGARWAL T M, SRIVASTAVA C. Microstructure, morphology and electrochemical properties of ZnFe−graphene composite coatings [J]. Journal of Alloys and Compounds, 2019, 783: 820−827.

[21] AMIRAT S, REHAMNIA R, BORDES M, CREUS J. Zn−Fe alloy electrodeposition from chloride bath: Influence of deposition parameters on coatings morphology and structure [J]. Materials and Corrosion, 2013, 64(4): 328−334.

[22] CHU Q W, LIANG J, HAO J C. Facile fabrication of a robust superhydrophobic surface on magnesium alloy [J]. Colloids and Surfaces A: Physicochemical and Engineering Aspects, 2014, 443: 118−122.

[23] ISHIZAKI T, SHIMADA Y, TSUNAKAWA M, LEE H, YOKOMIZO T, HISADA S, NAKAMURA K. Rapid fabrication of a crystalline myristic acid-based super-hydrophobic film with corrosion resistance on magnesium alloys by the facile one-step immersion process [J]. ACS Omega, 2017, 2(11): 7904−7915.

[24] KHORSAND S, RAEISSI K, ASHRAFIZADEH F, ARENAS M A, CONDE A. Corrosion behaviour of super-hydrophobic electrodeposited nickel−cobalt alloy film [J].

Applied Surface Science, 2016, 364: 349−357.
[25] ZHANG Y H, LIU J W, OUYANG L G, LI J M, XIE G E, YAN Y Y, WENG C. One-step preparation of robust superhydrophobic foam for oil/water separation by pulse electrodeposition [J]. Langmuir, 2021, 37(23): 7043−7054.
[26] MANOJ T P, RASITHA T P, VANITHAKUMARI S C, ANANDKUMAR B, GEORGE R P, PHILIP J. A simple, rapid and single step method for fabricating super-hydrophobic titanium surfaces with improved water bouncing and self cleaning properties [J]. Applied Surface Science, 2020, 512: 145636.
[27] LI L J, ZHANG Y Z, LEI J L, HE J X, LV R, LI N B, PAN F S. A facile approach to fabricate superhydrophobic Zn surface and its effect on corrosion resistance [J]. Corrosion Science, 2014, 85: 174−182.
[28] WU W C, CHEN M, LIANG S, WANG X L, CHEN J M, ZHOU F. Superhydrophobic surface from Cu−Zn alloy by one step O_2 concentration dependent etching [J]. Journal of Colloid and Interface Science, 2008, 326(2): 478−482.
[29] SOLOMON M M, UMOREN S A, QURAISHI M A, SALMAN M. Myristic acid based imidazoline derivative as effective corrosion inhibitor for steel in 15% HCl medium [J]. Journal of Colloid and Interface Science, 2019, 551: 47−60.
[30] ZHANG F, JIANG Y J, WU Z H, SONG J J, XU C Y, SHI Z W, PENG C S. Super-hydrophobic surface transferred from BTL using one step replication [C]//International Conference on Manipulation, Manufacturing and Measurement on the Nanoscale (3M-NANO). Changchun, China: IEEE, 2015, 263−266.
[31] FERNANDEZ A, FRANCONE A, THAMDRUP L H, JOHANSSON A, BILENBERG B, NIELSEN T, GUTTMANN M, SOTOMAYOR TORRES C M, KEHAGIAS N. Hierarchical surfaces for enhanced self-cleaning applications [J]. Journal of Micromechanics and Microengineering, 2017, 27(4): 045020.
[32] SUTAR R S, GAIKWAD S S, LATTHE S S, KODAG V S, DESHMUKH S B, SAPTAL L P, KULAL S R, BHOSALE A K. Superhydrophobic nanocomposite coatings of hydrophobic silica NPs and poly(methyl methacrylate) with notable self-cleaning ability [J]. Macromolecular Symposia, 2020, 393(1): 1−5.
[33] SUTAR R S, KALEL P J, LATTHE S S, KUMBHAR D A, MAHAJAN S S, CHIKODE P P, PATIL S S, KADAM S S, GAIKWAD V H, BHOSALE A K, SADASIVUNI K K, LIU S H, XING R M. Superhydrophobic PVC/SiO_2 coating for self-cleaning application [J]. Macromolecular Symposia, 2020, 393(1): 1−6.
[34] TAN Q C, GAO Z M, YAN J A, XIA D H, HU W B. Effect of chloride ions in acid and salt solutions on self-repairing ability and corrosion performance of titanium dioxide−fluorosiloxane superhydrophobic coating [J]. Progress in Organic Coatings, 2020, 146: 105675.
[35] LIU C S, SU F H, LIANG J Z, HUANG P. Facile fabrication of superhydrophobic cerium coating with micro-nano flower-like structure and excellent corrosion resistance [J]. Surface and Coatings Technology, 2014, 258: 580−586.
[36] KHORSAND S, RAEISSI K, ASHRAFIZADEH F. Corrosion resistance and long-term durability of super-hydrophobic nickel film prepared by electrodeposition process [J]. Applied Surface Science, 2014, 305: 498−505.
[37] SHI T, KONG J Y, WANG X D, LI X W. Preparation of multifunctional Al−Mg alloy surface with hierarchical micro/nanostructures by selective chemical etching processes [J]. Applied Surface Science, 2016, 389: 335−343.
[38] HUANG J D, CAI P H, LI M M, WU Q, LI Q, WANG S Q. Preparation of CNF/PDMS superhydrophobic coatings with good abrasion resistance using a one-step spray method [J]. Materials, 2020, 13(23): 1−10.

电镀超疏水锌铁涂层对镁合金的腐蚀防护

孟 雪[1]，王晋磊[1]，张 杰[1,2]，牛宝龙[1,2]，高向华[1,2]，晏 泓[1,2]

1. 太原理工大学 材料科学与工程学院，太原 030024；
2. 太原理工大学 新材料界面科学与工程教育部重点实验室，太原 030024

摘 要：采用简单、低成本、环保的方法在化学性质活泼的镁合金表面制备超疏水的 Zn−Fe 合金涂层。首先，在中性甘油 Zn−Fe 电解液中得到 Zn−Fe 涂层。该电镀液绿色、成分稳定且对设备无腐蚀性。随后，通过螯合反应改性将肉豆蔻酸接枝到 Zn−Fe 涂层表面，获得具有花状微观结构的超疏水表面。制备的超疏水涂层的水接触角>150°，滑动角为 3°～4°。与裸镁合金相比，电沉积时间分别为 30 和 50 min 的两组超疏水镁合金样品的腐蚀速率降低了约 87%。这表明所制备的超疏水涂层表现出优异的自洁性、耐磨性和耐腐蚀性。

关键词：锌铁涂层；镁合金；接触角；滚动角；自清洁；耐磨性

(Edited by Wei-ping CHEN)